Journal of Applied Polymer Science

Thermoplastic polyurethane synthesis with modified montmorillonite prepared by torque rheometry: Investigation of morphological, thermal, chemical, and physical properties

Felipe Gustavo Ornaghi, Vinicios Pistor, Ricardo Vinícius Boff de Oliveira
Universidade Federal do Rio Grande do Sul, Porto Alegre, Rio Grande do Sul, Brazil
Correspondence to: R. Oliveira (E-mail: ricardo.oliveira@iq.ufrgs.br) and F. G. Ornaghi (E-mail: fgornagh@gmail.com)

ABSTRACT: In this study, samples of thermoplastic polyurethane (TPU) were synthesized by reactive processing in an instrumented batch mixer with 0, 1, 2, 5, and 10 wt % of organophilic montmorillonite (OMMT) clay. Fourier transform infrared spectroscopy confirmed the obtainment of TPU. Transmission electron microscopy showed several types of clay dispersion. Analysis by X-ray diffraction revealed modifications in the TPU microstructure, a reduction in the degree of crystallinity, and an increase in the crystal size. Dynamic mechanical properties showed that the incorporation of OMMT has a strong influence on the storage and loss moduli obtained for the TPU matrix. The incorporation of OMMT also altered the crystallization and thermal stability of the TPU. With the use of the Flynn–Wall–Ozawa method it was observed that the nanoclay had a higher apparent activation energy. The results obtained applying the Criado method indicated that the solid state reaction is essentially controlled by geometric contraction, random nucleation with one nucleus for each individual particle and diffusion. © 2015 Wiley Periodicals, Inc. J. Appl. Polym. Sci. **2015**, *132*, 42640.

KEYWORDS: clay; crystallization; degradation; kinetics; polyurethanes

Received 14 December 2014; accepted 15 June 2015
DOI: 10.1002/app.42640

INTRODUCTION

Because of its ability to alternate between hard and soft segments, thermoplastic polyurethane (TPU) (a linear block copolymer which has the processability of thermoplastics and elasticity of vulcanized elastomers) is a very attractive material since the morphology can be controlled, resulting in many synthesis routes and processing applications.[1–5] This phase separation between soft and hard segments takes place rapidly and simultaneously with polymerization, and results from the thermodynamic immiscibility between the rigid and soft phases, forming microphases bound together by covalent bonds.[6] Secondary bonds between the polymers chains, such as strong hydrogen bonds between the urethane groups and urea (hard segments), make the material hypothetically "vulcanized" or "crosslinked" at ambient temperature. When subjected to high temperatures, these secondary bonds are broken and the polymer changes to the melt state, when it can be processed as a thermoplastic polymer. After cooling, the hydrogen bonds between the urea groups and urethane linkages are regenerated and the material once again behaves like an elastomer.[7] TPU can be molded applying the traditional techniques used for thermoplastics, but the urethane group has low thermal stability, and these bonds dissociate and re-associate simultaneously above the temperature of thermal stability.[8]

With the advances made in the area of nanotechnology, many options have appeared to overcome deficiencies, such as those related to TPU, and the use of organoclays dispersed in polymers offers benefits such as the exfoliation of the layers, reinforcement of the materials in nanometric scale, and an improvement in the mechanical, physical (thermal and barrier), and chemical properties.[3,9–12] Polyurethane nanocomposites containing nanoclay have been gaining greater attention recently[3,9–13] and the thermal degradation of polyurethanes has been extensively investigated by several research groups.[14–20] However, in the reaction process, mixing is performed in the molten state and performed under shear stress, to achieve coupling between the polymer matrix and the load.[21] The aim of this study was to investigate a processing method where the layered silicate swells in the liquid monomer (or a solution of the monomer) to form interleaved sheets during the synthesis of the polymer, and it is not necessary to melt the polymer and then incorporate clay. A processing step is therefore avoided as the synthesis occurs simultaneously with the expansion of the clay layers. To evaluate the changes in the properties of the TPU, organophilic clay with hydroxyl end groups was added through polymerization by reactive processing in the synthesis of thermoplastic polyurethane using a torque rheometer. Measurements were performed to evaluate changes in the thermal, morphological, and viscoelastic properties and in the mechanisms

associated with TPU and nanocomposite degradation through reactive processing.

MATERIALS

The materials used in this study were Urecon 185 prepolymer (Coim, with 18% of free NCO), 1,4-butanediol (BDO, MCassab), and organophilic clay (Cloisite 30B) with terminal OH groups. These materials were used as received. The prepolymer was based on polyol polyester with 4,4 MDI. The material contained 65% of rigid phase, considered as the quantity of isocyanate and of chain extender related to the quantity of reagents of which the polyurethane is comprised. Thus, the quantity of free isocyanate and chain extender was considered.

METHODS

The synthesis temperature used in this study was based on a publication by Fiorio *et al.*,[22] where the author reported that 70 °C is the best synthesis temperature for this method of obtaining TPU, an increase in the synthesis temperature promoting branching and/or crosslinking and changing the crystal structure. The synthesis was performed on an instrumented torque rheometer using roller-type rotors counter-rotating at a speed of 60 rpm and a temperature of 70 °C for 60 min. The total volume of the rheometer chamber was 75 cm^{-3} and the total mass of each mixture was 60 g. The stoichiometry was calculated on the basis of the equivalents of isocyanate (NCO) and hydroxyl (OH) for the prepolymer and BDO, respectively (molar ratio NCO/OH = 1 : 1). A rate of 98% reacted NCO was maintained throughout the synthesis. The clay was dried for 24 h at 80 °C. The prepolymer was first added to the rheometer and the BDO was then incorporated with 1, 2, 5, and 10 wt % of (organophilic montmorillonite) OMMT. The amount of OMMT incorporated also maintained the molar ratio of NCO/OH = 1 : 1. The polymers were removed from the rheometer in the form of solids and molded by compression with a pressure of ½ ton at 105 °C for 5 min. In the next step, the polymers were post-cured at 90 °C for 24 h.

Sample Characterization

Thermogravimetric Analysis. The thermogravimetric analysis (TGA) (QA050—TA Instruments) was performed under an N^2 atmosphere (50 mL min^{-1}), from 25 °C up to 750 °C. Approximately 10 mg of each sample was used in each analysis at four different heating rates (5, 10, 20, and 40 °C min^{-1}). The results were used to obtain the activation energy of degradation (E_a) through the method of Flynn–Wall–Ozawa[23,24] and the degradation mechanisms using the Criado *et al.*[25] method.

To determine kinetic parameters of reactions, Flynn, Wall, and Ozawa proposed the isoconversional method, by thermogravimetric and differential scanning calorimetry curves, based on Doyle's method proposed for heterogeneous chemical reactions,[26] eq. (1):

$$\log(\varnothing)=\log\left(\frac{AE_a}{R}\right)-\log\Big(g\ \big(\alpha\ (T)\big)\Big)-2.315-0.4567\ \frac{E_a}{RT}\quad(1)$$

where $g(\alpha(T))$ is a conversion ratio, E_a is the activation energy, R is the gas constant, A is a pre-exponential, Ø is the heating rate, and T is the absolute temperature. The isoconversional method assumes that the reaction rate is a function only of the temperature; however, for different heating rates at a constant degree of conversion ($\alpha(T)$), a linear relationship can be observed by plotting log(ØΦ) versus T^{-1}, and the activation energy is obtained from the slope of the straight line.[27] With the Doyle approximation for a range of log $p(E_a/RT)$ values between $20 < E_a/RT < 60$, the integral $p(x)$ can be simplified and expressed as shown in eq. (2):

$$\log p\ \left(\frac{E_a}{RT}\right)\cong -2.135-0.457\ \frac{E_a}{RT}\quad(2)$$

According to these simplifications, the Flynn–Wall–Ozawa (FWO) equation can be applied in thermal degradation kinetics studies [eq. (3)].

$$\log g\ (\alpha)\cong\log\left(\frac{E_a}{RT}\right)-\log\varnothing-2,135-0,457\ \left(\frac{E_a}{RT}\right)\quad(3)$$

The FWO method uses different heating rates, where the degree of conversion α is represented by a linear function of log (Ø) versus $1/T$ and the apparent activation energy is obtained from the slope of the linear fit.[28]

Criado *et al.* proposed a method to determine the thermal degradation mechanism.[29] This method is based on solid state reactions, using a master curve represented by the function [eq. (4)]:

$$Z\ (\alpha)=\frac{\frac{d\alpha}{dt}}{\varnothing}\ \pi\ (x)T\quad(4)$$

where x is E_a/RT and $\pi(x)$ is a function obtained by integral approximation in relation to temperature. As the function $\pi(x)$ cannot be obtained in algebraic form $\pi(x)$ and the function $Q(x)$ was proposed, eq. (5) results in:

$$\pi\ (x)=Xe^xQ(x)\quad(5)$$

On combining eqs. (4) and (5), $Z(\alpha)$ can be defined as in eq. (6):

$$Z\ (\alpha)=f(\alpha)-\ g\ (\alpha)\quad(6)$$

By eq. (6), it is possible to derive the relation in eq. (7):

$$Z\ (\alpha)=\frac{da}{dT}\frac{E_a}{R}e^{\frac{E_a}{RT}}\ Q\ (x)\quad(7)$$

In the above equation, $x = E_a/RT$ and $Q(x)$ is an integral approximation that cannot be expressed in a simple analytical form. A rotational equation has been proposed for $Q(x)$ for values of $x > 20$, resulting in errors of less than $10^{-5\%}$, in this case, the fourth term is rotational,[28] as shown in eq. (8):

$$Q\ (x)=\ \frac{e^{-x}}{x}\left(\frac{x^3+\ 18x^2+\ 86x+96}{x^4+\ 20x^3+\ 120x^2+\ 240x+120}\right)\quad(8)$$

Through the use of eq. (7) it is possible construct the master curve $Z(\alpha)$, using different templates.[28]

Differential Scanning Calorimetry. The differential scanning calorimetry (DSC) analysis (DSC Q20—TA Instruments) was performed under an N^2 atmosphere (50 mL min^{-1}) using approximately 10 mg of each sample. The samples were initially cooled from ambient temperature to −20 °C (held for 5 min), heated to 260 °C (held for 5 min), cooled to −20 °C again (held

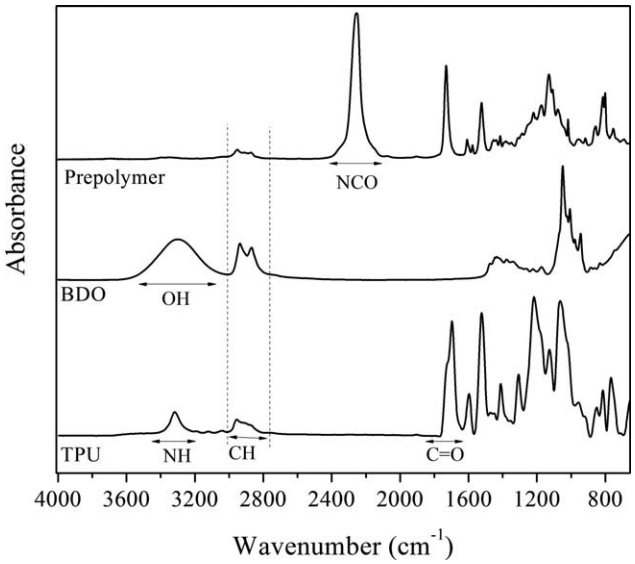

Figure 1. FTIR spectra for BDO, prepolymer and TPU.

for 5 min), and then heated back up to 260 °C. A heating rate of 10 °C min^{-1} was maintained for all the above steps.

X-ray Diffraction. X-ray diffractograms were collected using a sample holder mounted on a Siemens D500 diffractometer with monochromatic CuKα radiation ($\lambda = 0.15418$ nm). Intensities were measured in the range of $3 < 2\theta < 35°$, typically with scan steps of 2 s/step (1.5 ° min^{-1}). Peak separations were performed using Gaussian and Pseudo-voigt deconvolution. The *d* spacings were calculated using the Bragg equation[30] and the crystallite sizes (*L*) were calculated using the Scherrer equation.[8]

Dynamic Mechanical Analysis. The viscoelastic properties of the samples were characterized using a Q800 DMA multi-frequency-strain analyzer (TA Instruments) in single-cantilever mode and with rectangular specimens ($35 \times 10 \times 2$ nm^3). Tests were performed at a frequency of 1 Hz with a strain amplitude of 0.1%. The samples were heated from −90 °C to 200 °C at a heating rate of 3 °C min^{-1}.

Fourier Transform Infrared Spectroscopy. The Fourier transform infrared spectroscopy (FTIR) measurements were performed on a Bruker Alpha infrared spectrum analyzer in the wave-number range of 4000–600 cm^{-1}, at a resolution of 4 cm^{-1}.

Transmission Electron Microscopy. Transmission electron microscopy (TEM) images of the specimens were obtained using a ZEISS EM-922 OMEGA microscope with an operating voltage of 80 kV. The analysis was performed at −150 °C with a diamond knife.

RESULTS AND DISCUSSION

Reagents, Polymer, and Nanocomposite Characterization

The IR spectra in Figure 1 show the compositions of 1,4-butane diol (chain extender), the commercial prepolymer and the thermoplastic polyurethane obtained after the polymerization applying the reactive process. For the prepolymer, in the region of 2250 cm^{-1} the band is attributed to isocyanate and in the regions of 1730, 1608, 1570, and 1520 cm^{-1} to stretching of the C═O and N─H bonds.[31] For the chain extender, a broad and intense band can be observed in the region of 3300 cm^{-1}, attributed to OH groups, two absorption peaks in the region of 2937 and 2867 cm^{-1} correspond to CH groups and the band in the region of 1043 cm^{-1} is associated with the CO groups of alcohols. For the polymer, a band in the region of 3330 cm^{-1} is attributed to NH groups, a band at 1700 cm^{-1} to amide I (C═O axial strain) and a band in the region of 1530 cm^{-1} to the absorption of amide II (NH angular deformation). These bands suggest, in a preliminary qualitative analysis, that the polyurethane was successfully obtained. The band in the region of 2250 cm^{-1} observed for the prepolymer disappears on the spectrum for the polymer, and this absorption band is associated with free NCO groups. The disappearance of this peak in this region suggests the effective reaction between the prepolymer and the chain extender,[5] indicating that the reaction was successfully completed. Bands at 1300 cm^{-1} and 1060 cm^{-1} have stronger intensity in the case of the TPU compared with the prepolymer, due to the presence of ester groups in the polyol, which causes the enlargement of this absorption band, while for the prepolymer the absorption in this region is associated only with the C═O and C─O of urethane groups. The spectra for the nanocomposites were identical to those for the TPU, for all samples. No absorption was observed at around 2270 cm^{-1}, attributed to free NCO groups (unreacted), verifying conversion of the polymer, and also the bands associated with the formation of polyurethane were noted for all samples.[4,5,32] The incorporation of an increased amount of organoclay did not result in changes in the spectrum as the groups in the TPU and nanocomposites are identical. This suggests, in a preliminary qualitative analysis, that the segmented structure of TPU was not affected by the presence of organophilic clay, indicating that the modified silicate layers did not react with the TPU molecules, probably because organophilic clay is present in the system with many points of agglomeration.

Morphological Characteristics

The images in Figure 2 show the TPU has regions with clay sheets dispersed in exfoliated (EX), intercalated (IN), and agglomerated (AG) forms. The incorporation of 1 and 5 wt % of OMMT led to a mixed morphology, that is, with exfoliated to agglomerated regions. The incorporation of 10 wt % of OMMT led to a very poor dispersion in the polymer matrix, with many agglomerated regions. The poor dispersion of organophilic clay may result from the shear stress in the mixing chamber not being high enough, and hydrogen bonding between the polymer and the load did not occur efficiently, that is, the hydroxyl groups of the organophilic clay probably did not form hydrogen bonds with the hard segments of the TPU.

Four important diffraction peaks in the range $2\theta = 10$, 19, 21, and 23 ° (L_I, L_{II}, L_{III}, and LI_v, respectively) can be noted in Figure 3 for the TPU and nanocomposites. These diffraction peaks with interplanar spacings (*d*-spacing) of 0.84, 0.46, 0.41, and 0.37 nm are reportedly related to hard crystallized segments.[8,31] The peaks in the range of $2\theta = 19 - 23°$ relate to the hard crystalline segments of TPU (hydrogen bonds between urethane groups).[8] Peaks in the range of 2θ at approximately 10 ° are

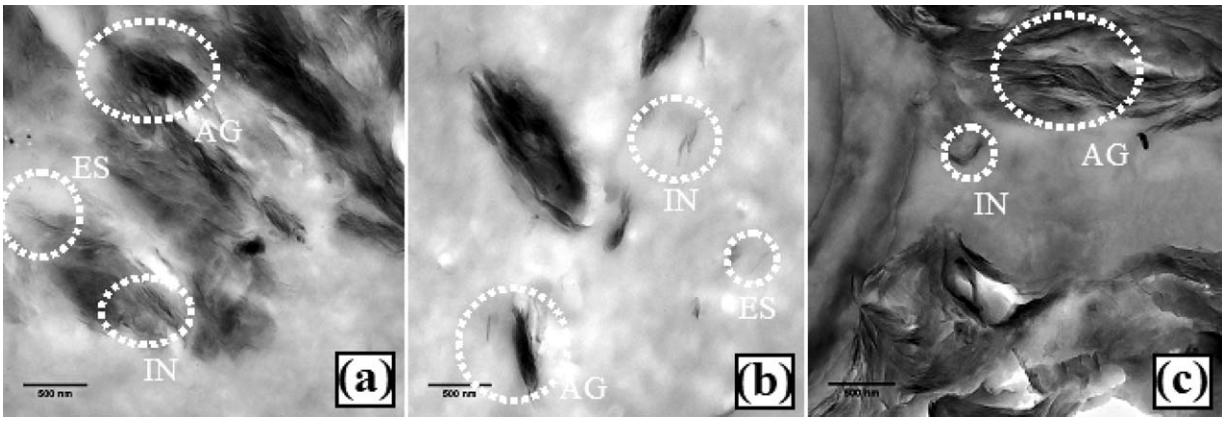

Figure 2. Images obtained by transmission electron microscope(TEM) for the samples: (a) TPU 1%; (b) TPU 5%; (c) TPU 10% (AG = agglomerates, EX = exfoliated, and IN = intercalated).

associated with the crystallinity of the hard segments and/or segments perpendicular to the surface of the lamellae.[8] MDI-based polyurethane usually forms hard segments that lead to phase separation.[33] The presence of Cloisite 30B was confirmed in the scanning range of $2\theta = 2.5°$ and $5°$,[3,5,11,34–37] where the peak observed in the region of $2.5°$ is an indication that the polymer chains are intercalated between the layers of organophilic clay.[36–38] The peaks corresponding to $2\theta = 2.5°$ for the nanocomposites have a greater interplanar distance than that of the organoclay ($2\theta = 5°$; interplanar distance $d = 1.8$ nm) due to the polymer being intercalated among the galleries of the nanoclay layers and thus the basal spacing increases.[37–39] The peak observed at $5°$ is due to the presence of agglomerates or organophilic tactoids in the nanocomposites. In the reflection range of $2\theta \approx 5°$, the diffraction peak corresponding to a *d*-spacing of 1.7 nm, which is the nanocomposite peak with the lowest intensity, indicates a new arrangement due to the incorporation of organoclay into the system. An increase in the intensity of these peaks with an increase in the organophilic clay content can be attributed to a greater quantity of montmorillonite in the system. The higher peak for the sample with 5% of organoclay compared with the peak for that with 10% may indicate the intercalation or partial exfoliation of the organoclay in the polymer, as noted in the TEM images. Barrick and Tripathy[3] attributed good intercalation or exfoliation to the interaction force of the hydrogen bonding between the polymer and the load. Hydroxyl groups of the clay are capable of forming hydrogen bonds with the hard segments of TPU. From the X-ray diffraction (XRD) diffraction results, it can be noted that polymerization by the reactive process was not sufficient to promote the full exfoliation of the organoclay in the TPU nanocomposites and only partial intercalation and exfoliation of samples occurred, although mostly agglomeration was observed, as noted in the TEM analysis. Through the calculation of the crystallite size using the Scherrer equation,[8] it was possible to evaluate the influence of OMMT domains in the crystalline structure of the TPU. The results for the determination of the crystal size are detailed in Table I. The incorporation of OMMT increased the crystallite size (L) compared with the neat TPU. This may occur because the crystals originated from the organoclay particles and were dispersed as agglomerates, as noted in the TEM analysis, favoring the formation of larger crystals and/or due to the presence of few exfoliated regions, a larger space between the sheets promoting the growth of larger crystals. The degree of crystallinity,[40,41] calculated from the XRD analysis, is shown in Table II where a decrease in the values can be observed with the incorporation of organoclay. This can be explained by the dispersion of montmorillonite, which probably increased the free volume of the system, consequently enhancing the molecular mobility, disturbing the system and not allowing the formation of many crystals, leading to less order in the system. For the samples with 10% of montmorillonite, it was not possible to measure the degree of crystallinity as there were no defined peaks. These results corroborate those obtained in the infrared spectroscopy and TEM, where the clay appeared to be

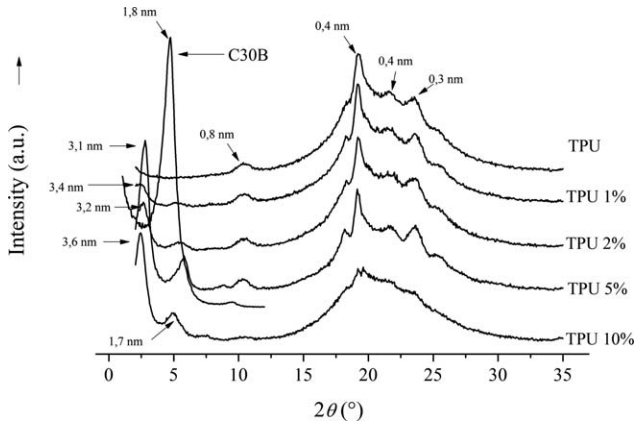

Figure 3. XRD patterns for TPU and nanocomposites.

Table I. Crystallite Sizes Obtained Applying the Scherrer Equation

Sample	L_I (Å)	L_{II} (Å)	L_{III} (Å)	L_{IV} (Å)
TPU	45.66	68.53	22.46	22.84
1%	59.59	85.66	41.53	42.83
2%	76.14	76.14	36.06	39.16
5%	76.14	97.9	25.86	80.62
10%	-	-	-	-

Table II. DSC Results for TPU and Nanocomposites and the Degree of Crystallinity Obtained by XRD

Sample	T_g Flexible Phase (°C)	T_g Rigid Phase (°C)	T_m (°C)	ΔH_m (J g^{-1})	X_c (%)	Crystallinity by XRD (%)
TPU	51.5	139.7	215.2	30.7	15	52 ± 5
TPU 1%	54.3	113.4	217.8	29.1	14	41 ± 4
TPU 2%	51.3	149.7	217.9	24.7	12	38 ± 4
TPU 5%	66.9	166.7	223.2	20.9	10	33 ± 2
TPU 10%	59.7	155.6	217.7	6.1	3	-

mostly agglomerated, which does not promote very effective reactions with the TPU molecules, favoring the reactions between the layers of organic silicate and this does not significantly influence the segment structure of the TPU.

Viscoelastic Properties

Storage Modulus. In Figure 4 it can be noted that the plateau in the vitreous region has a greater tendency to decrease with an increase in the temperature in the case of the nanocomposites compared with the neat TPU. The incorporation of organoclay can promote molecular disorientation in the nanocomposites, resulting in a decrease in the storage modulus for the vitreous region. The lowest value was observed for the neat TPU, as there is no interface at which to transfer the applied stress from the matrix to the nanofiller. Higher initial values were noted for the nanocomposites, which can be attributed to an attractive interaction of the hydrogen bonds between the carbonyl groups of the hard segment with the hydroxyl group present on the surface of organoclay.[12] This may indicate that the organoclay has a strong effect on the elastic properties of the TPU, due to a restriction of the molecular motion.[13] With an increase in the temperature, the E' values for all materials decreased due to an increase in the molecular mobility of the polymer chains.

Above the glass transition temperature, the samples containing 2, 5, and 10% of organoclay presented an increase in the mobility of the TPU chains, decreasing the E' values. This behavior may be associated with a decrease in the molecular arrangement of the rigid phase. Molecules dispersed in the rigid phase can also act as an impurity, decreasing the degree of crystallinity. As noted from the XRD results for the degree of crystallinity, higher values for the nanoclay lead to lower values for the crystalline percentage, resulting in less restriction in the molecular motion. Although the organoclay restricts the movement of the polymer chains,[3,12,13] there was a decrease in the E' values for nanocomposites in comparison to the neat TPU with increasing temperature, indicating that the nanoclay did not effectively enhance the elastic properties of the polymer. This observation is due to the fact that there are many agglomerations of nanoclay, as noted from the TEM results.

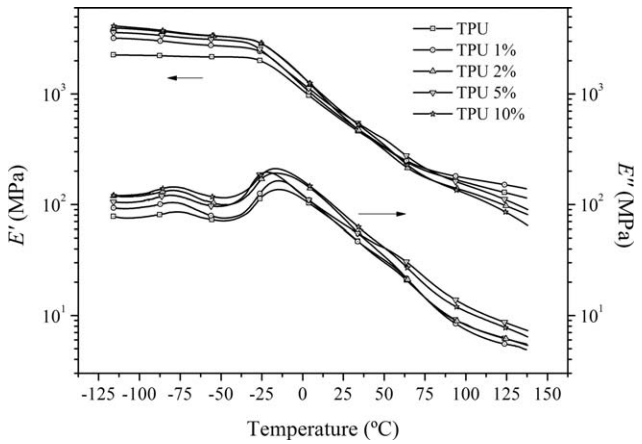

Figure 4. Storage (E′) and loss (E″) moduli versus temperature for all samples at a frequency of 1 Hz.

Loss Modulus. The values for the loss modulus (E'') show a similar behavior for all samples, but in the region of −75 °C the nanocomposites show a higher E'' value compared with the neat TPU. The transition observed in this temperature region is related to a β transition, due to the motion of the ester group of the flexible segments. The glass transition temperature in this region remained almost the same with the incorporation of montmorillonite, suggesting that montmorillonite does not interact with the ester group in the flexible phase, with inhibition of the relaxation process occurring as a result of the incorporation of the organoclay. At around −15 °C, the introduction of organophilic clay leads to a narrower and less intense transition, indicating that the presence of the nanoclay reduces the molecular mobility of the system due to a lower dissipation of energy. The loss modulus represents the response to plastic deformation,[3] which is related to the viscous response of the material. The behavior of the sample with 10% of nanoclay differed from that of the other samples. It is possible that in large quantities the nanoclay cannot be homogeneously dispersed in system and in this regard the TEM analysis revealed the formation of many agglomerates.

Tan Delta. In Figure 5, the behavior noted at −76 °C shows that with an increase in the amount of organophilic clay there is an increase in the peak heights. The peak height is an indication of how much energy will be dissipated in the system, high values indicating a weak interface in composites and nanocomposites.[42] Thus, if the reinforcement is effective, part of the tension will be absorbed by the material and the remaining energy will be dissipated as heat until reaching the interface created by the nanofillers. The nanocomposites showed a higher peak height in comparison with the neat TPU, which indicates that the nanoclay may act in the dispersed form in the system, as corroborated by the TEM results. For the reinforcement to be effective part of the tension should be shared by the reinforced material and the remaining energy will be dissipated in the

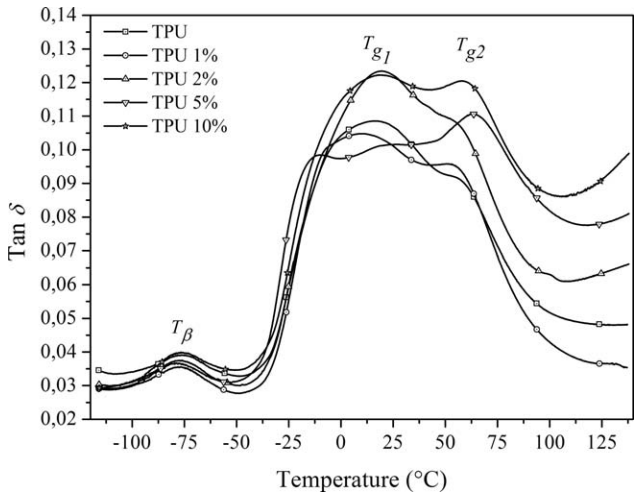

Figure 5. Tan δ curves obtained from the moduli in Figure 4.

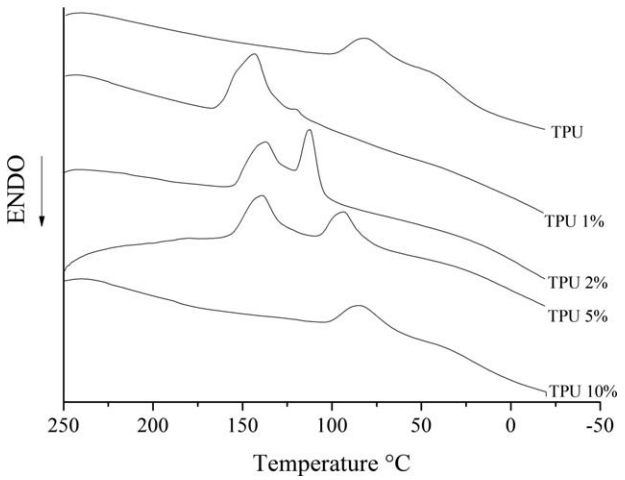

Figure 7. DSC thermograms for the cooling for all samples.

form of heat at the interface created by the nanofillers. However, this is not observed on the graph, as the nanocomposites release more energy than the neat TPU. This can probably be explained by the reaction between the hydroxyl group of montmorillonite and the hydroxyl group of the TPU not being effective, and/or because the system presents some degree of interleaving, increasing the basal spacing, as noted from the XRD results, where more energy can accumulate between the platelets of the nanoclays, which become larger as the quantity of montmorillonite increases. This region is attributed to the mobility of the ester groups present in the flexible segments. The peak width at half height varies according to the homogeneity of the system. A wide distribution reflects a considerable difference in the chain segment relaxation times and a narrow width corresponds to a small difference. The nanocomposites showed an enlargement of the curves as the percentage of nanoclay increased, as the organoclay affects the mobility of the nanocomposites. A more uniform system will require less molecular cooperativity and for the neat TPU, having a smaller curve, less effort is required for this phenomenon to occur, as no organoclay is present in the system. This is also an indication that the difference in the distribution of the relaxation times for the nanocomposites may be greater, due to the presence of montmorillonite in the system, which hinders the relaxation of the chain segments through their intercalation and exfoliation, as previously observed in the XRD and TEM results. The transition α, associated with the glass transition temperature for the flexible phase, showed a similar behavior for all samples, but with broader higher peaks for the nanocomposites. The peaks presented a bimodal form, with the major peaks varying according to the sample and secondary peaks appearing at approximately 45 °C. Two glass transition temperatures for the flexible phase were altered, which may be related to an increase in the molecular weight; however, it was not possible to test this hypothesis. The bimodal distribution of the relaxation times is attributed to slow and fast relaxations which, with the incorporation of clay, affect the mobility of the segments of the polymer backbone.[43]

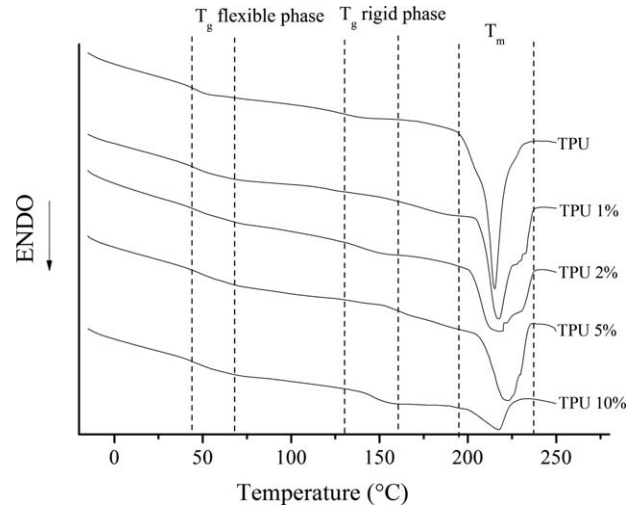

Figure 6. DSC thermograms for the first heating for the TPU and the nanocomposites.

Differential Scanning Calorimetry

Figure 6 and Table II show the thermographs and the results for the first DSC heating, respectively, for the TPU and the nanocomposites. The melting temperature of close to 200 °C is associated with the crystals formed by the rigid chain segments of the TPU, the crystallite structure of the hard segments of long-range order[44] becoming disordered with the incorporation of organoclay. Lower values for the enthalpy of fusion were found and this effect is probably due to a reduction in the quantity of TPU present, decreasing the amount of rigid segments in the mixture. In the temperature range of 44–70 °C the T_g for the flexible phase is observed, a similar temperature range being found by dynamic mechanical analysis (DMA), the difference in the values being due to the distinct characteristics of the techniques. Some authors refer to this transition as the second transition, in which short-range interactions within the rigid crystallite phase and interactions between the rigid phase and the flexible occur, these being associated with the T_g for the flexible phase being a negative temperature. The T_g for the rigid phase lies in the temperature range of 110–170 °C. During the

Table III. DSC Thermograms Obtained During the Cooling of the TPU and the Nanocomposites

Sample	T_c (°C)	ΔH_c (J g^{-1})
TPU	79.7	14.3
TPU 1%	143.3	11.9
TPU 2%	119 and 138.9	4.9 and 5.2
TPU 5%	93.3 and 138	4 and 7.8
TPU 10%	83.7	5.7

Table IV. DSC Thermograms for the Second Heating for the TPU and the Nanocomposites

Sample	T_m (°C)	ΔH_m (J g^{-1})
TPU	47.7 and 176.2	8.9 and 5.5
TPU 1%	183 and 220.5	2.2 and 14.5
TPU 2%	182, 204.2, and 219.9	2.3, 1.5 and 3
TPU 5%	180.5 and 213.5	2.8 and 4.1
TPU 10%	52 and 177.4	5.4 and 10.4

crystallization process, an increase in the mobility of the chains can occur. As the organoclay did not show good dispersion, the interface between the rigid and flexible phases may have been maintained. Also, the crystallinity values decreased with an increase in the montmorillonite, as shown by the crystallinity data obtained by XRD, the organoclay being dispersed in the system and providing no ordering for the growth of crystals.

Figure 7 and Table III show the results related to the crystallization during the cooling of the samples. The presence of two crystallization peaks in the samples with 1, 2, and 5% of the organoclay may be related to the formation of crystals of different sizes and/or the presence of crystallizable domains of different sizes. The crystallization peak for the neat TPU sample is wide, indicating that the crystals are formed in a more heterogeneous and/or imperfect manner. The shifting of the crystallization temperature to higher values for the samples with nanoclay in comparison to the neat TPU was also verified, which could be related to the presence of rigid structures in system that act as nucleation sites, allowing the formation of crystallizable domains of different sizes and with different crystallization temperatures. Also, residual crystals were present after the first heating, which can act as crystallization nuclei. The enthalpy of crystallization values for the nanocomposites was lower than those for the neat TPU, due to the incorporation of organoclay affecting the crystallization of the samples, as noted in the XRD analysis.

Figure 8 and Table IV show the DSC thermograms for the second heating of the samples. The first heating cycle presents a thermal–mechanical history, which can promote changes in the behavior observed by DSC, but for all other thermal cycles the modification may be associated with the dissociation and reassociation of urethane groups, where the thermal behavior of the sample changes due to its exposure to temperatures above the melting temperature. The nanocomposites had lower enthalpy of fusion values, indicating that the presence of montmorillonite leads to phase separation of the hard segment. The double peaks presented by the nanocomposites are attributed to the disordering of both types of crystallites in the hard segment, that is, type I (high degree of phase mixing) and type II (strong phase separation).[45]

Thermogravimetric Analysis

Table V shows the thermal degradation parameters obtained for the TPU, nanocomposites, and nanoclay. The TGA results for the neat TPU and the nanocomposites in Figure 9(a,b) show two stages of degradation, corresponding to the rigid and flexible phases. The first mass loss occurs in the range of 250–360 °C and this phase is attributed to the rigid phase (urethane groups). The second mass loss occurs in the range of 360–460 °C and is attributed to the phase flexible (polyol).[8,15,46] The samples remained stable up to a temperature of approximately 250 °C. With the incorporation of organophilic clay at higher percentages, both the hard and soft phases showed a decrease in the initial degradation temperature, which may be because the reactive end groups do not interact effectively with the surface of the inorganic nanoparticles, hindering the formation of hydrogen or covalent bonds. The decomposition of the organic modifier may have led to the collapse of organophilic particles

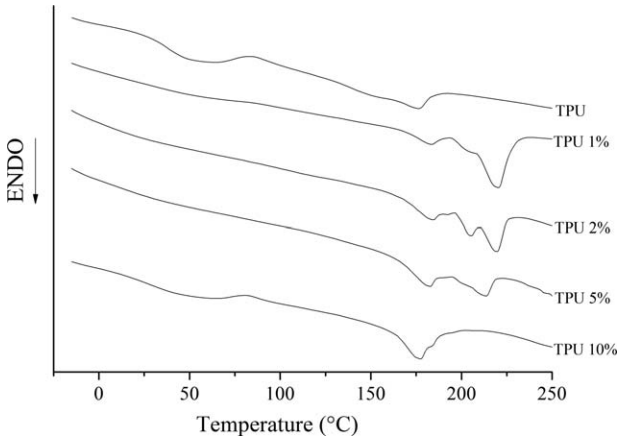

Figure 8. DSC thermograms for the second heating for all samples.

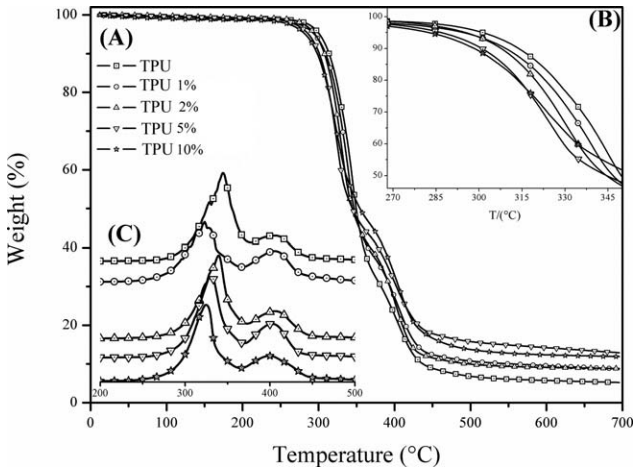

Figure 9. (a) TG and (b) DTA curves for nanocomposites.

Table V. TGA Results Obtained at a Heating Rate of 10 °C min^{-1} for the TPU, Nanocomposites, and Nanoclay

Sample	$DTG_{1máx}$ (°C)[a]	$DTG_{2máx}$ (°C)	T_{d1} (°C)[b]	T_{d2} (°C)	Residue (%)
TPU	344.4	405.2	278.2	374.9	5.2
TPU 1%	339.1	406.6	267.5	370.3	8.7
TPU 2%	330.5	403.3	265.6	369.1	8.9
TPU 5%	323.9	400.6	267.3	363.8	12
TPU 10%	323.2	405.9	252.7	366.7	17.9
OMMT	-	-	-	-	76.3

[a] DTG_{1max} (°C) = maximum degradation rate.
[b] T_{d1} (°C) = onset temperature.

due to an excess of agglomerates, affecting the thermal stability of the nanocomposites,[47] which probably influenced the decrease in the storage modulus with increasing temperature for the nanocomposites. The acceleration of the degradation process on incorporating organoclay into a polymeric system has been previously observed by other authors.[5,6,48,49] The DTG curves showed more clearly the two different decomposition processes, where the decomposition of phases occurs in a more independent manner, and lower values were obtained for the rigid phase.

The TGA analysis revealed that the incorporation of the nanofiller promoted a decrease in the initial degradation temperature for the rigid (urethane) and flexible (polyol) phases of TPU. A likely explanation for the decrease in the thermal stability of the first mass loss with an increased quantity of montmorillonite, may be an increased number of easily formed, less stable urethane groups, which results in a decrease in the thermal stability, as the initial degradation temperature for the urethane bond is dependent on the type of isocyanate and glycol used.[14,50] The presence of the organophilic clay may result in a higher ordering in the hard segments and the formation of more interurethane hydrogen bonds.[4] Monteavaro *et al.* demonstrated that the thermal stability of polyurethanes was dependent on the number of urethane groups per unit volume.[47]

After the first decomposition step, where the weakest polyurethane bonds are broken, the second and/or third degradation stages occur, which are dependent on the structure of the flexible segment and the three-dimensional arrangement. With the use of infrared spectroscopy, Chattopadhyay demonstrated that the rupture of the weakest bond (C—NH) has an activation energy of approximately 98 kJ mol^{-1}, corresponding to the first stage of degradation, and the initial degradation temperature for the urethane bond is dependent on the structure of the isocyanate and alcohol used.[14] According to Pattanayak,[5] a probable reaction mechanism can be described as follows: some polymer chain ends with —NCO groups diffuse to the vicinity of the clay galleries during the nanocomposite preparation and react with the $—CH_2CH_2OH$ group of the quaternary ammonium ions to produce urethane linkages (—CO—NH—). Another possibility is that the C=O groups of the hard segments of the polyurethane chains residing in the vicinity of clay particles form hydrogen bonds with the $—CH_2CH_2OH$ groups of the quaternary ammonium ions.

As the initial degradation temperature is lower for the organoclay than for the TPU, an evolution of the degradation process can be considered.[31] The first stage of degradation involves the thermal decomposition of the intercalated polymer, especially the polymer present on the surface of clay galleries. The nanocomposite degrades during this first stage of degradation more rapidly than the neat polymer, which may be due to the degradation of small molecules between the layers.[37] The decrease in the thermal stability of the corresponding flexible phase could be due to the incorporation of the nanofiller increasing the functionality of the polyol, which would result in a decrease in the thermal stability of flexible phase.[47] At this stage, the degradation is attributed to the rest of the intercalated polymer and also to the rest of the salt present between galleries of the clays.[37]

Regarding the thermal excitation, the covalent bonds of the polyurethane chains undergo vibration and rotation in a local space. This excitation may lead to the breakage of these chains and the formation of a variety of radical fragmented or small molecules, which can mutually recombine or undergo further fragmentation. This fragmentation can be of the vaporized (undergoing diffusion) or carbonized type. The thermal decomposition of polyurethane follows a similar route to random chain scission, with scission at the end of the chain and crosslinking.[14]

Mechanism of Decomposition

The E_a values obtained applying the FWO method are shown in Figure 10, where the trend toward higher E_a values for the samples containing montmorillonite can be observed. This behavior may be due to agglomerations of montmorillonite, noted in the TEM analysis, or to confinement of the organophilic sheet, requiring higher activation energy as the polymer chain undergoes a decrease in molecular mobility, as indicated by the loss modulus and tan δ results obtained by DMA. The agglomerates formed can modify the polymerization kinetics, increasing the values for the activation energy of polymerization. The dispersion of the organophilic clay can lead to an increase in the E_a value due to the restriction of the molecular segments and/or because the silicate layers serve as a barrier, slowing the heating

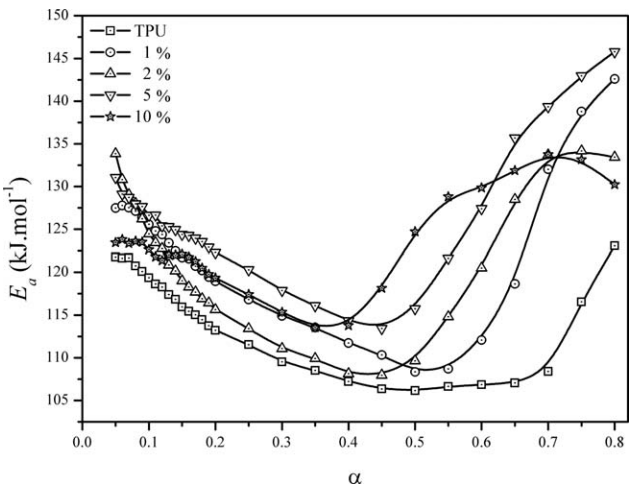

Figure 10. Activation energies obtained using FWO method.

of the hard segment.[3] However, this does not promote an increase in the thermal stability. The incorporation of organoclay may thus have led to restrictions that reduce the concentration of elastic chains and more thermal energy is needed to start the process of moving segments (molecular cooperativity), as noted from the tan δ values for the nanocomposites.

All samples showed a trend toward a decrease in the E_a values until around $\alpha = 0.4$. This finding can be explained by the heat generated by the reaction itself, as well as the catalytic effect of the urethane groups formed. Above this conversion value, the E_a values tended to increase because of the restricted movement and diffusion of molecules with the increased viscosity of the system.

Figure 11 shows the $Z(\alpha)$ results obtained applying the Criado method. The mechanisms of decomposition observed until around α 0.30 are R1, R2, R3, and F1, which involve surface-controlled reactions in three dimensions, corresponding to type Rn and random nucleation with one core for each individual particle (F1). At above α 0.45 the samples tend to show a diffusive behavior (Dn). Polymeric materials tend not to present only one mechanism of degradation as they do not display homogeneity in their molecular structure. The type Rn model considers geometric contraction, where the rate of degradation is controlled by the reaction occurring from the interface to the center of the sample, that is, nucleation occurs rapidly on the sample surface. This causes a reduction in the remaining area/volume which contains only organoclay. The organic molecules are primarily consumed, which may explain the finding that the TPU (Figure 10) tended toward a diffusive mechanism (Dn) when the conversion rate was higher than that of the nanocomposites, because there is no inorganic particles in the system. After a given conversion rate, the materials tend to adhere to a diffusion model, demonstrating that the degradation no longer occurs in a heterogeneous manner.

CONCLUSIONS

In this study, a thermoplastic polyurethane and organophilic montmorillonite Cloisite 30B nanocomposite was prepared by reactive processing, and the morphological, viscoelastic and thermal properties, and crystalline structure of the material obtained were investigated. The method used involved the formation of layers swollen in the solution of a molten silicate monomer, resulting in more finely dispersed sheets and rendering the organoclay the effective part of the final structure of the polymer.

Spectroscopic measurements were used to investigate the microstructure of the TPU and determine whether it is affected by the addition of the organophilic clay. It was observed that the synthesis conditions were favorable for obtaining thermoplastic polyurethane, and a reduction in the peaks for the urethane groups indicated that the reaction between the prepolymer and butanediol was complete.

X-ray diffraction analysis showed the formation of new crystalline phases with the incorporation of the organoclay, besides a decrease in the degree of crystallinity of the nanocomposites

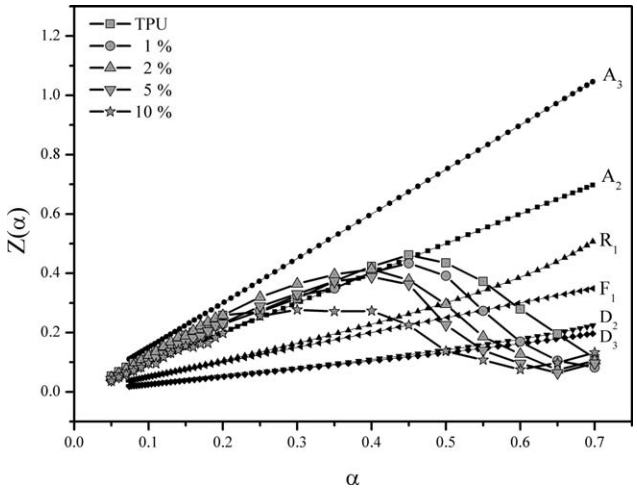

Figure 11. Experimental curves obtained applying the Criado *et al.* method.

and an increase in the amount of crystals due to the dispersed organoclay resulting in the unordered formation of crystals.

The dispersion of the nanoclay, observed through the transmission electron microscopy analysis, revealed the formation of sheets of organoclay dispersed in the thermoplastic polyurethane in an intercalated, exfoliated, and agglomerated manner. This was mainly due to the torque rheometer not having a high degree of shear and/or ineffective bonding of the polymer/filler bonds. For concentrations of up to 5% organoclay, the dispersion showed some points of exfoliation and intercalation; however, for the sample with 10% of montmorillonite, many agglomerated regions were observed.

The dynamic mechanical analysis shows α and β transitions and also the influence of organoclay as a reinforcing material, resulting in an increase in the initial storage modulus, the value for nanocomposites being lower than that for the TPU after a certain temperature, as the addition of clay reduces the thermal stability of the nanocomposites, as observed by TGA. Graphs of the elastic modulus values showed a trend toward more energy being dispersed in the system for the nanocomposites due to poor dispersion, as observed by TEM. The tan δ showed the reinforcing effect via enlargement of the curves, indicating the need for greater reinforcement in order for molecular cooperativity to occur, as the organoclay restricts some movement of the polymer chain segment.

The incorporation of montmorillonite into the thermoplastic polyurethane caused significant changes in the thermal properties of the material, mainly a decrease in the thermal stability of the TPU, which resulted in more sensitivity in terms of the melting and crystallization processes, when exposed to temperatures above the melting point, modifying the degradation mechanisms due to the presence of organoclay in the system.

Through the kinetic study it was possible to verify that the incorporation of montmorillonite increased the activation energy values and the mechanism of degradation for all samples followed a trend involving a reaction controlled by the phase boundary (Rn), random nucleation with one nucleus for each

individual particle (F1), and nucleation and growth (A2) up to a conversion rate α of 0.30 while diffusion (Dn) was observed above a conversion rate α of 0.45.

The production of TPU/montmorillonite nanocomposites through reactive processing causes changes in the microscopic and macroscopic behavior of the thermoplastic polyurethane, which are mainly a response to the degree of dispersion and the reactions occurring in the system.

ACKNOWLEDGMENTS

The authors gratefully acknowledge UFRGS and Brazilian National Counsel of Technological and Scientific Development (CNPq) for their scholarships and financial support.

REFERENCES

1. Zia, K. L.; Bhatti, H. N.; Bhatti, I. J. *React. Funct. Polym.* **2007**, *67*, 675.
2. Madbouly, S. A.; Otaigbe, J. U. *Prog. Mater. Sci.* **2009**, *34*, 1283.
3. Barick, A. K.; Tripathy, D. K. *Polym. Adv. Technol.* **2010**, *21*, 835.
4. Dan, C. H.; Kim, Y. D.; Lee, M.; Min, B. H.; Kim, J. H. *J. Appl. Polym. Sci.* **2008**, *108*, 2128.
5. Pattanayak, A.; Jana, S. C. *Polymer* **2005**, *46*, 5183.
6. Agic, A.; Bajsic, E. G.; Rek, V. J. *Elastom. Plast.* **2006**, *38*, 105.
7. Ionescu, M. In Chemistry and Technology of Polyols for Polyurethanes; Rapra Technology: Shawbury, Shrewsbury, Shropshire, **2005**; Chapter 1, p 6.
8. Pistor, V.; De Conto, D.; Ornaghi, F. G.; Zattera, A. J. *J. Nanomater.* **2012**, *212*, 1.
9. Cervantes, J. M.; Espinosa, J. M.; Cauich-Rodriguez, J. V.; Ortega, A.; Torres, H.; Fernandez, A.; Roman, *J. Polym. Degrad. Stabil.* **2009**, *94*, 1666.
10. Mishra, A. K.; Chattopadhyay, S.; Rajamohanan, P. R.; Nando, G. B. *Polymer* **2011**, *52*, 1071.
11. Meng, X.; Wang, Z.; Yu, H.; Du, X.; Li, S.; Wang, Y.; Jiang, Z.; Wang, Q.; Tang, T. *Polymer* **2009**, *50*, 3997.
12. Barick, A. K.; Tripathy, D. K. *Appl. Clay Sci.* **2011**, *52*, 312.
13. Barick, A. K.; Tripathy, D. K. *Mater. Sci. Eng.* **2010**, *527*, 812.
14. Chattopadhyay, D. K.; Webster, D. C. *Polym. Sci.* **2009**, *34*, 1068.
15. Bikiaris, D. *Thermochim. Acta* **2011**, *523*, 25.
16. Herrera, M.; Matuschek, G.; Kettrup, A. *Polym. Degrad. Stabil.* **2002**, *78*, 323.
17. Lage, L. G.; Kawano, Y. J. *Appl. Polym. Sci.* **2001**, *79*, 910.
18. Seymor, R. W.; Cooper, S. L. *Macromolecules* **1973**, *6*, 48.
19. Levchik, S. V.; Weil, E. D. *Polym. Int.* **2004**, *53*, 1585.
20. Barendrect, R. B.; Berg, P. J. *Thermochim. Acta* **1980**, *38*, 181.
21. Begshev, V. P.; Malkin, A. Y. Reactive Process of Polymers; Chem Tec: Toronto, **1999**.
22. Fiorio, R.; Pistor, V.; Zattera, A. J.; Petzhold, C. L. *Polym. Eng. Sci.* **2012**, *52*, 1678.
23. Ozawa, T. *Data Bull. Chem. Soc. Jpn.* **1965**, *38*, 1881.
24. Flynn, J. H.; Wall, L. A. J. *Res. Natl. Bur. Stand.: A. Phys. Chem.* **1966**, *70A*, 487.
25. Criado, J. M.; Malek, J.; Ortega, A. *Thermochim. Acta* **1989**, *147*, 377.
26. Doyle, C. D. *Nature* **1965**, *207*, 290.
27. Bianchi, O.; Oliveira, R. V. B.; Fiorio, R.; Martins, J. D. N.; Zattera, A. J.; Canto, L. B. *Polym. Test.* **2008**, *27*, 722.
28. Bianchi, O.; Castel, C. D.; Oliveira, R. V. B.; Bertuoli, P.; Hilling, E. *Polímeros* **2010**, *20*, 395.
29. Pérez-Maqueda, L. A.; Criado, J. M. J. *Anal. Calorim.* **2000**, *60*, 909.
30. Halasa, A. F.; Wathen, G. D.; Hsu, W. L.; Matrana, B. A.; Massie, J. M. *J. Appl. Polym. Sci.* **1991**, *43*, 183.
31. Trovati, G.; Sanches, E. A.; Neto, S. C. *J. Appl. Polym. Sci.* **2010**, *115*, 263.
32. Chen, T. K.; Tien, Y. I.; Wei, K. H. *Polymer* **2000**, *41*, 1345.
33. Mittal, V. *Materials* **2009**, *2*, 992.
34. Paiva, L. B.; Morales, A. R.; Díaz, F. R. V. *Cerâmica* **2008**, *54*, 213.
35. Meng, X.; Du, X.; Wang, Z.; Bi, W.; Tang, T. *Compos. Sci. Technol.* **2008**, *68*, 1815.
36. Leite, I. F.; Raposo, C. M. O.; Silva, S. M. L. *Cerâmica* **2008**, *54*, 303.
37. Rehab, A.; Salahuddin, N. *Mater. Sci. Eng. A* **2005**, *399*, 368.
38. Tien, Y. I.; Wei, K. H. *Polymer* **2001**, *42*, 3213.
39. Alexandre, M.; Dubois, P. *Mater. Sci. Eng.* **2000**, *28*, 1.
40. Carvalho, A. P.; Carvalho, M. B.; Pires, J. *Elsevier Sci.* **1997**, *19*, 382.
41. Foner, H. A.; Adan, N. *J. For. Sci. Soc.* **1983**, *23*, 313.
42. Pistor, V.; Ornaghi, F. G.; Ornaghi, H. L.; Zattera, A. J. *Mater. Sci. Eng. A* **2012**, *532*, 339.
43. Qazvini, N. T.; Mohammadi, N. *Polymer* **2005**, *46*, 9088.
44. Frick, A.; Rochman, A. *Polym. Test.* **2004**, *23*, 413.
45. Fiorio, R.; Zattera, A. J.; Ferreira, C. A. *J. Appl. Polym. Sci.* **2009**, *112*, 2896.
46. Qin, H.; Zhang, Z.; Feng, M.; Gong, F.; Zhang, S.; Yang, M. *J. Polym. Sci. Part B: Polym. Phys.* **2004**, *42*, 3006.
47. Monteavaro, L. L.; Silva, E. O.; Costa, A. P. O.; Dimitrios, G.; Annelise, E.; Petzhold, C. L. J. *Am. Oil Chem. Soc.* **2005**, *82*, 365.
48. Xu, X.; Ding, Y.; Qian, Z.; Wang, F.; Wen, B.; Zhou, H.; Zhang, S.; Yang, M. *Polym. Degrad. Stabil.* **2009**, *94*, 113.
49. Labidi, S.; Azema, N.; Perrin, D.; Lopez-Cuesta, *J. Polym. Degrad. Stabil.* **2010**, *92*, 382.
50. Song, Y. M.; Chen, W. C.; Yu, T. L.; Linliu, K.; Tseng, Y. H. *J. Appl. Polym. Sci.* **1996**, *62*, 827.